Collective nature of two-dimensional electron gas spin excitations revealed by exchange interaction with magnetic ions

P. Barate, S. Cronenberger, M. Vladimirova, and D. Scalbert
Groupe d'Etude des Semi-conducteurs, UMR 5650 CNRS, Université Montpellier 2, Place Eugène Bataillon, 34095 Montpellier Cedex, France

F. Perez, J. Gòmez, and B. Jusserand
Institut des nanosciences de Paris, UMR 7588 CNRS, Université Paris 6, 140 rue de Lourmel 75015, Paris

H. Boukari, D. Ferrand, H. Mariette, and J. Cibert
Institut Néel, CNRS-Université Joseph Fourier, BP 166, 38042 Grenoble Cedex 9, France

M. Nawrocki
Institute of Experimental Physics, University of Warsaw, Hoża 69, PL-00-681 Warszawa, Poland
(Received 2 June 2010; revised manuscript received 16 July 2010; published 9 August 2010)

Time-resolved Kerr rotation experiments in CdMnTe quantum wells provide the evidence of mixed spin excitations of the two-dimensional electron gas and magnetic ions. The onset of strong coupling between electron and Mn spin modes reveals the collective (spin-wave) nature of electronic spin excitations probed by this method. We show that resonant exchange coupling between electron-spin waves and magnetic ions spin-flip excitations provide insights in the many-body physics of the two-dimensional electron gas.

DOI: 10.1103/PhysRevB.82.075306 PACS number(s): 75.50.Pp, 73.21.−b, 78.47.J−

I. INTRODUCTION

The existence of collective spin excitations in a two-dimensional electron gas (2DEG) is one of multiple manifestations of many-body interactions.[1] Collective spin excitations such as spin waves formed by intersubband spin transitions,[2,3] as well as spin-splitted fractional Hall states[4] have been intensively studied in last years. Such excitations and their dispersion have been observed in different materials, such as Si-, GaAs-, and CdTe-based structures. Studies of collective spin excitations of a 2DEG in the time domain has been less reported in the literature. Recently, Bao *et al.*[5] were able to identify long-wavelength intersubband spin waves in the time-resolved Kerr rotation signal, by comparison with Raman spectra.

A completely new piece of information on the spin excitations of a spin-polarized 2DEG was brought by Ref. 6. This work investigates the intrasubband spin excitations of a 2DEG confined in a diluted magnetic semiconductor (DMS) quantum well. The spin excitation spectrum of a DMS involves both itinerant *s*-type electron (or *p*-type hole) spins and spins localized on the magnetic (Mn^{2+}) ions. The two systems are coupled together by the exchange interaction.[7] In a (Cd,Mn)Te quantum well, an in-plane magnetic field of moderate intensity (~3 T) polarizes the spins localized on the magnetic ions. Even for low Mn concentrations (~0.2%), this enables a strong spin splitting of the 2DEG, without any substantial orbital quantization, a configuration which is unaccessible in conventional semiconductors. This makes the electron-spin splitting large enough to be observed by means of optical spectroscopy. Raman spectra reported in Ref. 6 provide the evidence of both collective and individual spin excitations of the spin-polarized 2DEG.

It was also shown that, according to Larmor theorem, collective 2DEG spin excitations with zero wave vector have the frequency given by the spin splitting of one *isolated* electron (i.e., the bare giant Zeeman splitting) while the individual modes (or single-particle excitations) lie at higher frequency due to many-body effects (Fig. 1). Comparing the individual and collective spin mode frequencies allowed measuring the enhancement of the 2DEG spin polarization due to electron-electron interactions.[8]

The spin excitation spectrum of a DMS like (Cd,Mn)Te or (Ga,Mn)As involves both itinerant *s*-type electron (or *p*-type hole) spins and spins localized on the magnetic (Mn^{2+}) ions, the two systems being coupled together by the exchange interaction.[7] In (Ga,Mn)As, the much larger coupling be-

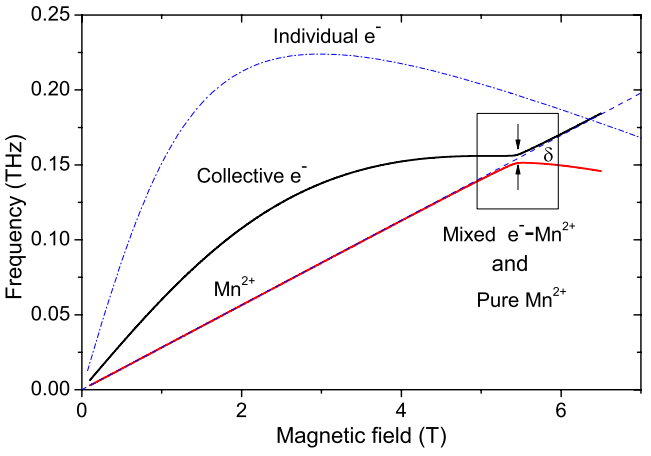

FIG. 1. (Color online) Schematic representation of spin precession modes in *n*-doped (Cd,Mn)Te quantum wells. The anticrossing between the collective electron mode (spin wave) and Mn spin excitations at $g_m=2$ is indicated in the rectangular frame. Other excitations of the 2DEG, such as spin-density waves and charge-density waves based on intersubband excitations, sit at higher energy.

tween free carriers (holes in the valence band) and Mn spins deeply alters the Mn spin excitations, as described, e.g., in Ref. 9. Then spin waves appear as a result of the carrier-induced ferromagnetic coupling between the Mn spins. A softening of the collective mode at the ferromagnetic transition was predicted[10] and experimentally observed in *p*-type (Cd,Mn)Te quantum wells.[11,12] The spin-carrier coupling is smaller in the case of conduction electrons so that the excitation of the Mn spins in an *n*-doped (Cd,Mn)Te quantum well is usually observed[13] simply at $g_m=2$.

Note that the term "spin waves" was used above to describe two different objects: spin waves formed in the 2DEG thanks to electron-electron interactions and spin waves formed in the system of localized spins due to the interaction through the free carriers.

Although in *n*-type diluted magnetic quantum wells the exchange coupling is smaller, under some conditions it can also alter Mn spin excitations. It was shown previously that in *n*-doped (Cd,Mn)Te quantum wells the application of a magnetic field may create resonant conditions, such that the frequency of the electron-spin precession is close to that of the Mn spin precession. Under such conditions the *s-d* exchange interaction between the conduction electrons and the magnetic ions results in the strong coupling between the spin precession modes of electrons and magnetic ions (Fig. 1). The corresponding anticrossing was observed with the field applied out of plane, by Raman scattering and electron paramagnetic resonance,[14] and described theoretically.[9,15] It was shown that the anticrossing is due to the transverse (or "dynamic") part of the exchange interaction between carriers and Mn; the splitting is directly related to the spin polarization of the 2DEG, which was estimated from the occupation of Landau levels.

Further work[16] demonstrated that these strongly coupled mixed electron-Mn spin modes can be observed in the time domain by Kerr rotation, with the field applied in plane (hence, no orbital quantization) and that these collective modes coexist with pure Mn spin excitations, which appear at $g_m=2$ in the gap between the collective modes. A theory based on coupled Bloch equations for the average electron spin and individual Mn spins was used to explain both mixed and pure Mn spin modes.[16] This theory, as that of Ref. 15, integrates out the conduction-band degrees of freedom, hence it ignores the many-body properties of the electron gas.

In this work, we apply the time-resolved Kerr rotation technique to study the electron-Mn spin excitations in a set of four (Cd,Mn)Te quantum wells with different values of the electron density. We use the Bloch equations describing the mixed modes[16] with the spin polarization of the 2DEG as a unique adjustable parameter.

We show that: (i) only collective spin excitations of the 2DEG (long-wavelength electronic spin waves), and not single-particle excitations, strongly couple to the Mn spin excitations and contribute to the Kerr rotation signal.

(ii) In view of the strong spin relaxation of the electronic spin-wave mode observed, the achievement of strong-coupling conditions (real anticrossing) can be understood only by taking into account electron-electron interactions and the resulting enhancement of the spin polarization of the 2DEG. This enhancement of the spin susceptibility favorably compares with theories[17] which consider a 2DEG without orbital quantization. Actually, our quantitative data even suggest a slightly stronger enhancement.

(iii) Under such strong-coupling conditions, a collective mode is imprinted into the Mn spin system; an orthogonality condition is proposed for the noncoupled Mn modes, which were observed in three of the four samples under study.

Thus, the mixed electron-Mn modes are collective in two senses (i) due to carrier-carrier interactions, as in Ref. 6 and (ii) due to electron-Mn interactions, as in Refs. 9 and 14–16.

The carrier-carrier interactions play a decisive role in the energy of spin excitations in the long-wavelength limit: as shown in Ref. 15 the anticrossing energy gap is proportional to the electron-spin polarization ζ, which is known to be strongly affected by the density-dependent Coulomb interactions within the 2DEG. This is a case of breakdown of the Larmor theorem due to the fact that the spin-carrier exchange couples two systems characterized by different Landé factors. We will come back to that point later on.

The paper is organized as follows. The next section recalls how the spin dynamics in a diluted magnetic quantum well under in-plane magnetic field is described by the coupled Bloch equations. From these equations one can see that only collective spin excitations of 2DEG may strongly interact with the magnetic ion spins. From their solutions we obtain the explicit formula for the spin polarization of the 2DEG ζ as a function of the anticrossing gap. Time-resolved Kerr rotation study of the spin excitations in four (Cd,Mn)Te *n*-doped samples is presented in the Sec. III. Finally, we compare the 2DEG spin-polarization enhancement extracted from our experiments with the existing theoretical predictions (Sec. IV).

II. MODEL

In this section we recall the main results obtained in Ref. 16 and show that (i) the existence of a strong coupling between electron and Mn spin excitations reveals the collective nature of the electron-spin mode and (ii) how the spin polarization of the 2DEG can be recovered from the experimentally measured anticrossing gap.

Let us consider a 2DEG, characterized by the sheet density n_e, confined along the x direction in a DMS quantum well of width w. We limit ourselves to the lowest quantization subband, where electron envelope function along the quantization direction is $\chi(x)$. The electron gas interacts with the Mn ions with spin $J=5/2$, characterized by the sheet density n_m. The exchange constant is noted α. The magnetic field $\mathbf{B}$ is applied in the plane of the structure in the direction z and the equilibrium spin components $\mathbf{S}_z$ for the electrons and $\mathbf{J}_z$ for the Mn spins are assumed to be much larger than the corresponding transverse components $\mathbf{S}_\perp$ and $\mathbf{J}_\perp$ which will appear within the spin excitations. In this case, and using the fact that Mn spins within a monolayer (a same crystallographic plane of the quantum well) are identical, the linearized Bloch equations can be reduced to a set of $N+1$ equations, N being the number of monolayers in the quantum well.[16] The transverse component of the averaged electron

spin $\mathbf{S}_\perp$ is coupled to the N transverse components of Mn spins averaged within each monolayer, $\mathbf{J}_{\perp,n}$,

$$\frac{d\mathbf{S}_\perp}{dt} = -(\mathbf{S}_\perp \times \mathbf{\Omega}_e) + \frac{\Delta}{J_z}\frac{w}{N}\sum_{n=1}^{N}(\chi_n^2 \mathbf{J}_{\perp,n} \times \mathbf{S}_z) - \frac{\mathbf{S}_\perp}{\tau_e}, \quad (1)$$

$$\frac{d\mathbf{J}_{\perp,n}}{dt} = -(\mathbf{J}_{\perp,n} \times \mathbf{\Omega}_m) + \frac{Kw}{S_z}\chi_n^2(\mathbf{S}_\perp \times \mathbf{J}_z). \quad (2)$$

The first term in each Eqs. (1) and (2) accounts for the precession of the transverse spin component in the effective magnetic field given by sum of the external field and the exchange field. Thus the corresponding precession vector is $\hbar\mathbf{\Omega}_m = g_m\mu_B\mathbf{B} + K\mathbf{S}_z/S_z$ for Mn spins and $\hbar\mathbf{\Omega}_e = g_e\mu_B\mathbf{B} + \Delta\mathbf{J}_z/J_z$ for electron spins. Here $\Delta = -\alpha n_m J_z/w$ is the giant Zeeman energy (mean-field exchange energy acting on the electron spins due to the Mn spins) and $K = -\alpha n_e S_z/w$ is a Knight shift (mean-field exchange energy acting on the Mn spins due to the 2DEG). Note that $K \ll \Delta$ by two to three orders of magnitude; actually the exchange part of the effective field acting on Mn spins is much smaller than the external field, hence it can be safely neglected.

The equilibrium average spin of the magnetic ions J_z is known to be properly described by the so-called modified Brillouin function B_J for $J=5/2$, $J_z = -JB_J(g_m\mu_B B/k_B T_{eff})$, where T_{eff} phenomenologically accounts for the Mn-Mn interactions.[18] In contrast, the spin polarization of the 2DEG, $\zeta = (n_\uparrow - n_\downarrow)/n_e = 2S_z$, may be affected by the electron-electron interactions, and therefore, it will be kept as the unique fitting parameter of our model.

The third term in Eq. (1) phenomenologically accounts for the electron-spin relaxation with a characteristic time τ_e. The relaxation of Mn spins is orders of magnitude slower than the electron one so that it can be ignored.

The second terms in each Eqs. (1) and (2) are responsible for the dynamical coupling between spins. Here $\mathbf{J}_\perp \equiv (w/N)\Sigma_{n=1}^{N}\chi_n^2\mathbf{J}_{\perp,n}$ is the averaged nonequilibrium component of Mn spin, weighted by the probability $\chi_n^2 = \chi^2(x_n)$ to find the electron on the Mn lattice site x_n. It appears that the resonant coupling between electron and Mn spins is only possible if $S_\perp \neq 0$, which means that all the electrons precess with the same phase, that is, for a *collective* electron-spin precession mode. In contrast *individual* electron-spin excitations are characterized by a random distribution of the precession phase. Therefore, $S_\perp \approx 0$ so that the coupling term in Eq. (2) vanishes. Moreover, because the Kerr rotation signal from the 2DEG is usually supposed to be proportional to $\mathbf{S}_\perp$, we should not expect any substantial contribution from the individual spin excitations in our experiments. Thus, the electron-spin precession mode detected in the Kerr rotation experiments has to be identified as the lower collective spin excitation of the 2DEG detected at the same energy by Raman spectroscopy in Ref. 6. This is one of the important conclusions of this work.

The very existence of the collective spin mode in a 2DEG is due to spin-dependent Coulomb interaction between electrons. However, in the long-wavelength limit its frequency is equal to that of a single electron in the same magnetic field. This is a consequence of the Larmor theorem: in a system which is rotationally invariant, the Hamiltonian commutes with the total spin. Hence, if a magnetic field is applied, only the Zeeman effect contributes to the evolution of the total spin and if the system is formed of particles with a unique Landé factor, the evolution of the total spin is governed by the same Landé factor: this is the spin wave in the long-wavelength limit. Thus, no information about the many-body effects in 2DEG can be obtained directly from frequency of the collective spin mode, as far as Larmor theorem applies.

However, Larmor theorem is known to breakdown in case the Landé factor is not single valued. This is the case here since *s-d* exchange couples the 2DEG and the Mn spins which have different g factors (it is only the longitudinal part of the exchange which brings the excitation energies to the same values). Another point of view, quite popular in the field of DMS's, would be to integrate this longitudinal exchange interaction and consider an effective g factor or electrons but then, the transverse spin-carrier exchange which makes the coupling is no more isotropic and Larmor's theorem breaks down anyway. In all cases, it follows that the anticrossing energy can be used as a probe of the many-body effects in the 2DEG.

To see how this becomes possible, let us consider the $(N+1)$ solutions of Eqs. (1) and (2), as reported in Ref. 16. There are $(N-1)$ pure Mn modes and two mixed modes.

The pure Mn modes satisfy the conditions $\mathbf{J}_\perp = 0$ and $\mathbf{S}_\perp = 0$. They are all degenerate at the frequency Ω_m. The corresponding distribution of the transverse Mn spin across the quantum well is orthogonal to the distribution of the electron density χ_n^2 so that these modes are decoupled from the electron spin. This orthogonality condition, which is quite different from previous assumptions in a slightly different case,[9] emerges in a very straightforward way from Eqs. (1) and (2).

The two coupled electron-Mn spin modes correspond to the collective precession (either in phase or with the opposite phases) of the electron spins and Mn spins, described by $\mathbf{S}_\perp$ and $\mathbf{J}_\perp$. These modes involve complex eigenfrequencies $\omega_\pm$, given by

$$\omega_\pm = \frac{1}{2}\left(\Omega_e + \frac{i}{\tau_e} + \Omega_m\right) \pm \frac{1}{2}\sqrt{\left(\Omega_e + \frac{i}{\tau_e} - \Omega_m\right)^2 + 4\eta K\Delta/\hbar^2}, \quad (3)$$

where $\eta = w\int_0^w \chi^4(x)dx$. The quantity w/η can be considered as an effective width of the 2DEG, which also governs carrier-induced ferromagnetism in a DMS quantum wells.[19]

In $\omega_\pm$, the real parts are the spin mode precession frequencies while the imaginary parts are the corresponding decay rates. An anticrossing of the collective modes occurs [i.e., $\mathrm{Re}(\omega_+) \neq \mathrm{Re}(\omega_-)$ at resonance], if $\tau_e > \hbar/2\sqrt{\eta K\Delta}$. This is the so-called strong-coupling condition. Then the frequency gap δ between the modes reads

$$\delta = 2\sqrt{\eta K\Delta - \left(\frac{\hbar}{2\tau_e}\right)^2} \quad (4)$$

while at resonance the decay times of both modes are equal to $\tau_- = \tau_+ = 2\tau_e$. As the electron-spin polarization $\zeta = 2S_z$ enters the Knight shift K, we obtain

TABLE I. Samples parameters.

Samples	1	2	3	4
n_e (10^{11} cm^{-2})	1.34	2.4	2.85	2.9
x_{eff} (%)	0.24	0.29	0.25	0.27
w (nm)	10	15	10	12
η	1.15	1.27	1.15	1.2
T_{eff} (K)	2.9	6.1	4.2	5.35
B_0 (T)	5.9	5.4	5.9	5.6
τ_e (ps)	20	24	18	22
δ (μeV)	36	24	26	28
Δ (meV)	1.275	1.325	1.300	1.300
K (μeV)	0.4	0.22	0.29	0.27
ζ	0.8	0.38	0.26	0.3

$$|\zeta| = \frac{w\hbar}{\alpha n_e} \frac{\delta^2 + (\hbar/\tau_e)^2}{2\eta\Delta}. \tag{5}$$

In this expression, as will be shown below, δ, τ_e, and Δ can be directly measured in the time-resolved Kerr rotation experiment, w, η, and α are known structure parameters, and the nominal value of n_e can be refined using photoluminescence data. Therefore, in the following sections we use this result to measure the spin-polarization degree of the electron gas.

The model also provides the squared amplitudes of the electron contribution within the two collective mixed modes, to which the Kerr signal is believed to be proportional

$$A_- = \frac{D + \sqrt{\delta^2 + D^2}}{2\sqrt{\delta^2 + D^2}}, \tag{6}$$

$$A_+ = \frac{\delta^2}{2\sqrt{\delta^2 + D^2}(D + \sqrt{\delta^2 + D^2})}, \tag{7}$$

where $D = \Omega_m - \Omega_e$.

The behavior of the collective modes as a function of the in-plane magnetic field is fully characterized by the frequencies, relaxation times, and amplitudes reported above, providing a sound basis for the comparison with Kerr rotation experiments.

III. EXPERIMENT

A. Samples and experimental setup

We used four different samples grown by molecular-beam epitaxy, containing a single n-doped (Cd,Mn)Te quantum well with different values of the 2DEG density n_e, and slightly varying values of the well width ($w \approx 12$ nm) and Mn content ($x \approx 0.25\%$). The density n_e was determined from photoluminescence and Raman spectroscopy.[20] Sample parameters are summarized in Table I. The samples were placed in the liquid-helium cryostat at 2 K and a magnetic field was applied in the plane of the quantum well.

Spin excitations were created and detected using time-resolved Kerr rotation.[21] The train of 1 ps pulses was obtained from the Ti-sapphire laser by spatial filtering of the 100 fs pulses. The signal was optimized by tuning the wavelength of the laser close to the Fermi edge singularity at $\lambda \approx 764$ nm. The resulting beam was split into pump (0.2 mW) and probe (0.1 mW) beams, and both were focused on the 0.2 mm diameter spot on the sample surface. The circularly polarized pump pulse creates about 10^{10} cm^{-2} electrons and holes in the quantum well, spin polarized in the x direction which is perpendicular to the magnetic field. The density of the photocreated carriers is therefore at least one order of magnitude smaller than the density of the resident carriers and cannot modify significantly the quantum well properties. Also note that although the carriers are created with some distribution of kinetic energy, they are known to thermalize rapidly (within 1 ps) to the lattice temperature.

The heavy-hole contribution to the x component of the magnetization decays during a very short time about 5 ps.[22] But because the in-plane g factor of heavy holes is vanishing and their spin does not precess,[23] the effective magnetic field created by the holes during this initial short time rotates the spins of the magnetic ions away from the direction of the applied field. This is believed to initiate the precession of the Mn spins around the external field.[21] Altogether, the short circularly polarized pulse generates the precession of both Mn and electron spins around the magnetic field.

The spin polarization created by the pump pulse was detected using linearly polarized probe pulses: the rotation of the probe polarization after reflection from the sample is proportional to the x component of the electron spin. Finally, changing the delay between pump and probe pulses provides information on the dynamics of the x component of the total magnetization.

It is worth to remember that the contribution of the magnetic ions to the signal is not direct but mediated by the effect of the Mn spin polarization on the interband transitions.[24] Therefore, although Mn spin signal in (Cd,Mn)Te quantum wells has been detected in Kerr rotation experiments,[21] it can be hardly seen in samples with a low Mn content[25] such as those of the present study.

B. Results

Figure 2 shows the Kerr rotation signal observed at $B = 3$ T on samples 2 and 3. Sample 3 is the same sample as in Ref. 16.

For sample 2, the decaying oscillations involves a single, well-defined frequency, easily recognized in the power spectrum obtained by Fourier transformation (inset). From its dependence on the applied field value, it is attributed to the precession of the electron spins. The Mn spin signal at $g_m = 2$ could not be detected on this sample.

In contrast, on sample 3 we measure both the electron and Mn spin contributions. Indeed, although the electron-spin relaxation is much faster in this sample ($\tau_e = 7$ ps, compared to 19 ps in sample 2), a weak signal persists after complete relaxation of the electron spin. The frequency of this oscillation is slower than the electron-spin precession and it corresponds to the g factor $g_m = 2$. The amplitude of this Mn signal is nevertheless much smaller than the electron's one.

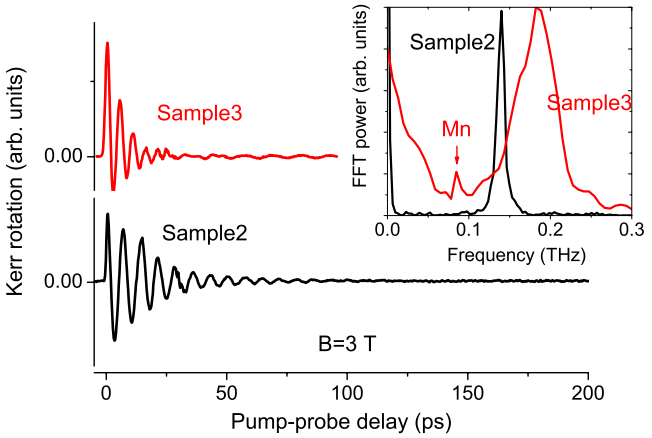

FIG. 2. (Color online) Time-resolved Kerr rotation scans measured at $B=3$ T for samples 2 (black line) and 3 (red line). Inset shows the corresponding Fourier spectra.

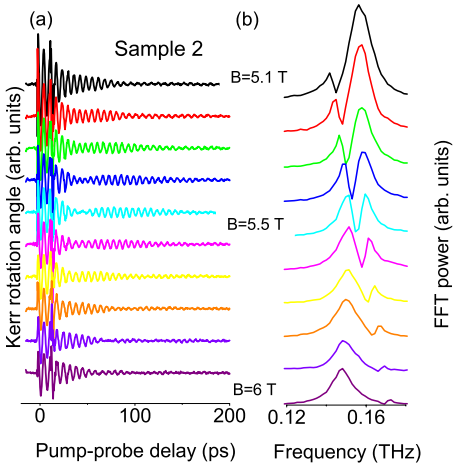

FIG. 3. (Color online) Waterfall plots (a) of the time-resolved Kerr rotation and (b) of the corresponding Fourier spectra, measured under magnetic field in the resonance region from $B=5.1$ T to $B=6$ T on sample 2.

We do detect both electron and Mn spin precessions in all our samples, except sample 2. Out of resonance ($B<5$ T), the electron-spin precession is faster than that of Mn. The spin-relaxation times are also very different: while the electron-spin-relaxation time τ_e never exceeds 30 ps, the relaxation time of the Mn spin mode, albeit difficult to determine precisely, is estimated to be on the order of 1 ns.

The measured values of τ_e are much shorter than in nonmagnetic semiconductor quantum wells. This is typical in DMSs, and it is generally accepted that in these systems electron-spin relaxation is governed by spin-flip scattering with Mn atoms, even if quantitative agreement with theory is still lacking.[22,26] We emphasize that existing theories apply to single-particle spin relaxation while we are measuring relaxation of collective spin excitations. When approaching electron-Mn spin-resonance conditions (about 5–6 T in all samples), the spin dynamics changes drastically.

Let us first describe results obtained on sample 2 where the Mn spin precession could not be detected out of resonance. In this sample, in contrast with the three other ones, pure Mn modes have not been detected even at resonance. This makes the description of the Kerr rotation signal in the anticrossing region simpler since the amplitude of the Mn-like collective mode is expected to be only given by its electronic component [Eq. (6)]. In addition, in sample 2 we obtained the longest electron-spin-relaxation time, and the lowest anticrossing field $B_0 \sim 5.5$ T, which allows for a more comprehensive exploration of both sides of the resonance, including the case where the Mn spin splitting exceeds that of electrons. Thus, we have chosen this sample to illustrate how the spin polarization of the electron gas can be extracted from our data.

Figure 3 shows waterfall plots of the Kerr rotation measured in the vicinity of resonance (magnetic field ranging from 5.1 to 6 T) together with the corresponding Fourier spectra. At $B=5.1$ T a second oscillating component already appears in the signal. Upon increasing the magnetic field, its amplitude grows up. At $B=5.5$ T a beats pattern is very apparent: at this point the two mixed modes have identical amplitudes which means that the anticrossing is reached. Further increase in the field brings us to the other side of the resonance: the Mn-like mode has a frequency higher than the electronlike mode, it looses progressively its weight and finally it is hardly seen at $B=6$ T.

For a quantitative treatment of these data, we fit the Kerr rotation curves using a superposition of two decaying cosine functions. Out of resonance this procedure yields the frequency and the spin-relaxation time of the electronic excitation. At resonance we extract the frequencies, relaxation times, and amplitudes of both mixed modes. The result is shown by symbols in Fig. 4 as a function of the applied field. Out of resonance, the electron frequency exhibits a typical Brillouin function behavior. This allows us a good determination of the parameters describing the DMS: temperature T_{eff} and effective spin concentration x_{eff}. The latter is related to the Mn spin sheet density n_m as $x_{eff}=n_m/wN_0$, where $N_0=1.46\times10^{22}$ cm^{-3} is the number of unit cells per unit volume in CdTe.

The electron-spin-relaxation time τ_e is another important ingredient of the model, as it enters the expression of the electron-spin polarization in Eq. (5). But Fig. 4 shows that τ_e varies significantly even out of resonance. Such a nonmonotonous behavior has already been observed and interpreted in terms of the nonhomogeneous heating of Mn^{2+} spins by the electron gas.[27] This suggests that a relevant value of τ_e, in order to describe the anticrossing, is that observed at strong field, where the Mn spins are almost saturated. For sample 2 we thus obtain $\tau_e=24$ ps.

Solid lines in Fig. 4 are our best fit of the data using Eq. (3) with the parameters summarized in Table I. The anticrossing of the frequencies as well as the crossing of the relaxation times and amplitudes are well described by the model. The fact that the amplitude of one of the modes goes to zero above and below the resonance confirms that Mn spins contribute to the Kerr rotation mainly as far as they are coupled to the electron spin. Also note that the relaxation time of the electronlike mode increases up to $2\tau_e$ due to the coupling with relaxation-free Mn spins: this is an intrinsic property of the model of coupled oscillators.

Let us now discuss sample 3, as one of the samples where Mn spin precession could be detected out of resonance. The

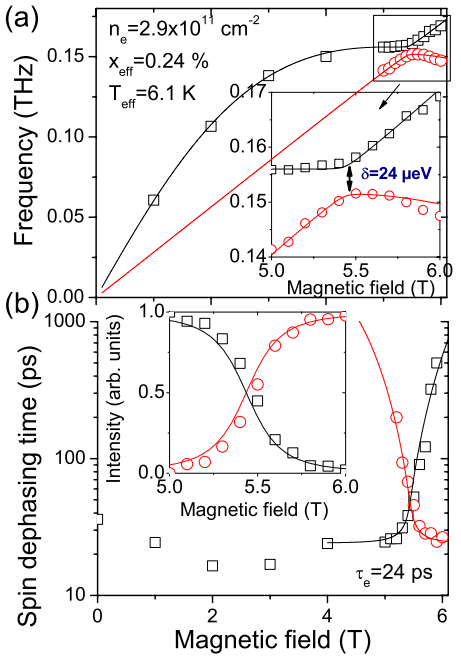

FIG. 4. (Color online) (a) Spin precession frequencies and (b) decay times extracted from Kerr rotation measurements under magnetic field $B=1-6$ T (sample 2). Insets show the frequencies (a) and the intensities $A_{\pm}$ of the two coupled modes in the resonance region defined in Eq. (6). Symbols show the experimental data, lines are the best fit obtained using Eq. (3) assuming the parameters listed in Table I.

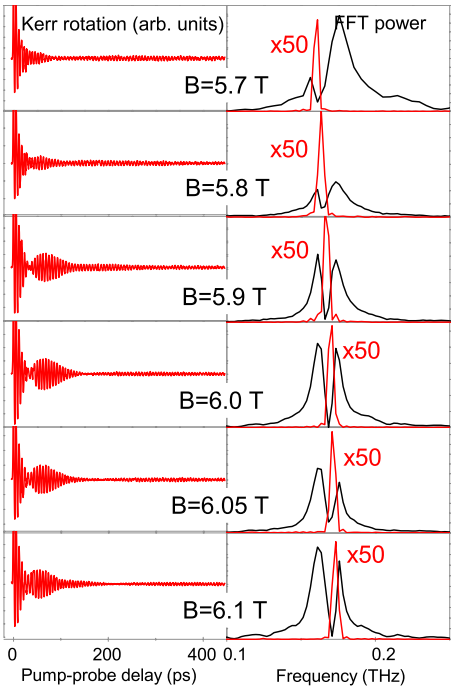

FIG. 5. (Color online) Time-resolved Kerr rotation scans (left panel) and the Fourier spectra (right panel) from sample 3 with magnetic field values ranging from 5.7 to 6.1 T (resonant conditions). Two Fourier spectra correspond to each measurement, one for the short delays ($0<t<225$ ps, black line) and the other for the long delays ($225<t<450$ ps, red line).

data obtained for this sample have been partly presented in the previous communication.[16] The left panel in Fig. 5 shows Kerr rotation scans measured for different fields in the vicinity of the resonance (which occurs at $B=5.9$ T). At short delays, $t<200$ ps, the oscillating signal exhibits beats, with a maximum at 5.9 T. At longer delays, only a low amplitude, long-living signal persists.

The Fourier spectra of these time scans are shown in the right panel of Fig. 5. In order to separate the long-living component from the mixed modes, for each magnetic field value we show two Fourier spectra corresponding to two different time windows. The first one, obtained from delays $0<t<225$ ps (black line), features the two modes which anticross when the magnetic field increases. These are the coupled electron-Mn modes. The second Fourier spectrum, for $225<t<450$ ps (red line, multiplied by the factor 50), shows the pure Mn spin excitation. Its frequency follows a linear dependence on the magnetic field and it is not affected by the resonance with electrons. Its amplitude is much lower than that of the collective modes, in agreement with the fact that Mn spin excitations do not interact directly with the light but only via carriers. As far as these excitations are decoupled from the conduction-band states, they can be detected only via valence-band states, provided that the symmetry of the hole envelope function differs from the electron one. Therefore, an asymmetry of the quantum well structure seems to be a prerequisite for the observation of the decoupled modes. In our samples this is achieved by the asymmetrical δ doping in the topmost barrier only.

In contrast, both mixed modes contain electron-spin contribution, and thus provide a much stronger Kerr rotation signal. The apparently higher amplitude at $B=5.7$ T and $B=5.8$ T is due to the poor separation between the lower frequency collective mode and the pure mode at these fields.

In order to get more accurate results, a fit of the time domain data by three damped cosine functions was used, as in Ref. 16. The only fixed parameter was the relaxation time of the pure mode $\tau_m=1$ ns because using time delays smaller than 450 ps does not allow for an accurate determination. Overall, we are able to identify the collective modes and recover their frequencies and relaxation times properly for all four samples. These results will be discussed in the next section.

IV. DISCUSSION

Figure 6 summarizes the experimental data on the dynamics of the collective modes. For the four samples under investigation, the frequency difference $(\omega_+-\omega_-)$ and the difference between the corresponding relaxation times $(\tau_+-\tau_-)$ are shown by symbols. The solid lines are the best fits realized using the procedure described above, using the parameters listed in Table I.

As a next step we use Eq. (5) to extract the electron-spin polarization ζ, which is shown by open squares in Fig. 7 as a function of the 2DEG concentration n_e. The vertical error bars are mainly determined by the uncertainty in the determination of τ_e and δ while the horizontal error bars were deduced from comparison between the values obtained from Raman and photoluminescence spectroscopy.[20]

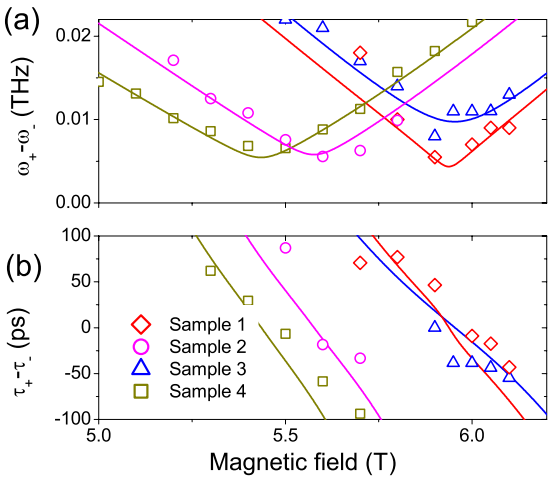

FIG. 6. (Color online) Differences between (a) the frequencies and (b) relaxation times of the mixed modes for samples 1 (diamonds), 2 (circles), 3 (triangles), and 4 (squares). Solid lines are best fit using Eq. (3) with parameters listed in Table I.

As expected, the experimental values largely exceed the polarization calculated for a noninteracting Fermi gas of the same density (open circles in Fig. 7). Indeed, it is well established that at low electron density, Coulomb interactions enhance the spin polarization of a paramagnetic electron gas over that of the noninteracting Fermi gas. In order to compare our data with the existing models, we plot the 2DEG spin-polarization enhancement as a function of the dimensionless spacing between electrons, $r_s=(a_B\sqrt{\pi n_e})^{-1}$, which controls the strength of the many-body effects. The result is shown in the inset of Fig. 7 in comparison with the theory of Attaccalite *et al.*[17] This model appears to fit some experimental results from the literature,[28] and even slightly overestimate the enhancement.[20,29] Note that the calculated spin polarization for a Fermi distribution is not significantly affected by the finite temperatures of the experiments. Hence, we can safely compare our results with the theory of Attac-

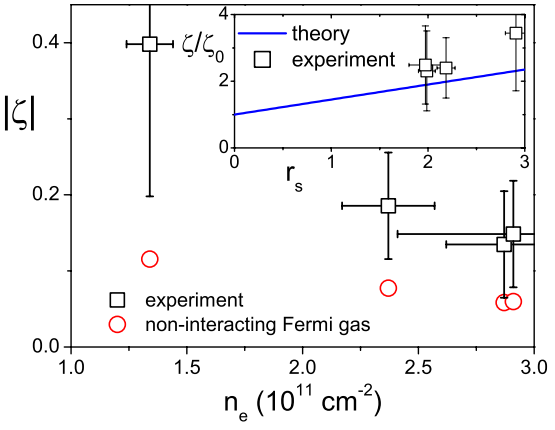

FIG. 7. (Color online) 2DEG spin polarization extracted from the anticrossing splitting using Eq. (5) (squares) and calculated assuming a Fermi distribution (circles), as a function of the 2DEG density. Inset shows the enhancement of the spin polarization with respect to the Fermi gas as a function of dimensionless spacing between electrons r_s. Solid line is the theory from Ref. 17.

calite *et al.* developed for $T=0$. In the range of r_s values of interest the spin-polarization enhancement can be approximated by $\zeta/\zeta_0=1+0.46r_s$. The calculated values stay within the error bars of our experimental values but show a systematic trend to underestimate the enhancement.

This is in contrast with Raman-scattering and PL experiments.[20] Note however that a direct comparison of the results obtained with both techniques is difficult because for practical reasons the samples studied in Ref. 20 are different from those studied here. It is also difficult to discuss the accuracy of one method compared to the other. Time-resolved Kerr rotation is at least as accurate as Raman scattering concerning the determination of the absolute energy of the modes. However, in Kerr rotation the determination of ζ relies on the anticrossing model for collective spin excitations, and hence could be model dependent.

We will discuss possible reasons for a systematic overestimation of ζ deduced from the Kerr rotation experiments. But first, it is important to stress that, using the parameters listed in Table I together with the value of the Knight shift K calculated from the theoretical values of the spin polarization ζ (solid line in Fig. 7), we get negative values under the square root in Eq. (4). This means that, for the theoretically expected values of the 2DEG spin-polarization enhancement, the electron-Mn strong-coupling condition would not be fulfilled for any of our samples.

One possible reason for an overestimation of ζ could be a wrong interpretation of the measured electron-spin-relaxation time τ_e. Indeed, in Eq. (4) it is assumed that the decay of the Kerr signal results from an homogeneous spin-relaxation mechanism characterized by τ_e. It might be due instead to an inhomogeneous distribution of electron-spin waves frequencies, arising, for example, from fluctuations in the local Mn spin concentration. We solved the problem of coupling of the Mn spins to either a Lorentzian or Gaussian distribution of the electron mode frequencies and found that the spin polarization does not differ significantly from the one obtained using the model of two coupled oscillators. Thus, our method for the spin-polarization determination appears to be robust with respect to the mechanism (homogeneous or inhomogeneous) of the electron dephasing.

It was shown that disorder and localization phenomena may alter the spin-polarization values deduced from magnetoresistance measurements.[30] Indeed, in the experiments of Piot *et al.*, the critical field needed to fully polarize the electrons was shown to be determined by the density of the delocalized states, rather than the total electron density. Although disorder is not expected to affect the optical experiments in the same way, the overestimation of the 2DEG density relevant for the electron-Mn coupling may lead to an underestimation of the polarization as well.

Finally, we note that our measurements are obtained under experimental conditions different from those of magnetotransport. In magnetotransport experiments the main method used to obtain the spin-polarization enhancement consists in measuring the value of the magnetic field, applied in the quantization direction, needed to fully polarize the 2DEG (filling factor $\nu=1$). The other method consists in determining the value of an oblique field, such that the spin splitting between Landau levels coincides with that of the

orbitally quantized Landau levels. Both imply the application of a strong magnetic field, orbital quantization, and a strong polarization of the 2DEG. However, as shown recently,[31] the renormalization of the spin polarization due to many-body effects is a nonlinear function of the magnetic field. This makes difficult a comparison of our results with that of magnetotransport experiments. Nevertheless, the strong point is that we do observe the strong-coupling regime, which implies a strong polarization enhancement, even if a fully quantitative explanation is still missing.

At this point it is not quite clear whether the disagreement between our experimental values of ζ and the theoretical ones, can be ascribed solely to experimental inaccuracies. On the theoretical side the effect of disorder is not included, and there is no general agreement on whether disorder should enhance,[32,33] or rather suppress the electron-spin polarization.[34]

V. CONCLUSIONS

Our study of the dynamics of spin excitations in *n*-doped (Cd,Mn)Te quantum wells shows that the anticrossing of the 2DEG and magnetic ions spin modes, as well as pure Mn spin modes, are systematically observed in the samples with different electron density. Theoretical consideration of the interaction between magnetic ions and different excitations of the 2DEG (spin waves and individual spin flips) allowed us to conclude that only collective spin excitations (spin waves) may strongly couple to the Mn spins. Based on this argument, we identified the electron-spin mode observed in Kerr rotation experiments as a collective one while individual spin-flip excitations do not appear in these experiments.

This conclusion is important for the understanding of the 2DEG spin dynamics. Indeed, our result suggests that time-resolved Kerr rotation, which is one of the most powerful techniques to study the spin dynamics of the 2DEG, does probe the collective excitations. This result does not depend on the presence of the magnetic ions in the quantum well. Therefore, taking into account the collective nature of the spin excitations may help understanding the 2DEG spin dynamics in both diluted magnetic and conventional semiconductor quantum wells.

The other important result of this work concerns the estimation of the 2DEG spin-polarization degree from the anticrossing between electron and Mn spin excitations. Resonant interaction with magnetic ions causes the Larmor theorem to breakdown so that long-wavelength collective 2DEG spin excitations reveal the many-body properties of the 2DEG, such as spin-polarization enhancement. However, the resulting spin-polarization values exceed systematically the values reported in the literature, suggesting that our understanding of the underlying physics is still not fully quantitative.

ACKNOWLEDGMENTS

We acknowledge helpful discussions with M. I. Dyakonov and A. P. Dmitriev, high quality samples from T. Wojtovicz, and financial support from the ANR project "GOSPIN-INFO." This work was partially supported by the Polish Ministry of Science and Higher Education as research grants in years 2008–2011.

[1] A. K. Rajagopal, Phys. Rev. **142**, 152 (1966).
[2] A. Pinczuk, S. Schmitt-Rink, G. Danan, J. P. Valladares, L. N. Pfeiffer, and K. W. West, Phys. Rev. Lett. **63**, 1633 (1989); D. Gammon, B. V. Shanabrook, J. C. Ryan, and D. S. Katzer, Phys. Rev. B **41**, 12311 (1990).
[3] J. C. Ryan, Phys. Rev. B **43**, 4499 (1991).
[4] P. Plochocka, J. M. Schneider, D. K. Maude, M. Potemski, M. Rappaport, V. Umansky, I. Bar-Joseph, J. G. Groshaus, Y. Gallais, and A. Pinczuk, Phys. Rev. Lett. **102**, 126806 (2009).
[5] J. M. Bao, L. N. Pfeiffer, K. W. West, and R. Merlin, Phys. Rev. Lett. **92**, 236601 (2004).
[6] B. Jusserand, F. Perez, D. R. Richards, G. Karczewski, T. Wojtowicz, C. Testelin, D. Wolverson, and J. J. Davies, Phys. Rev. Lett. **91**, 086802 (2003).
[7] J. Cibert and D. Scalbert, in *Spin Physics in Semiconductors*, edited by M. I. Dyakonov (Springer, Berlin, 2008), p. 389.
[8] F. Perez, C. Aku-leh, D. Richards, B. Jusserand, L. C. Smith, D. Wolverson, and G. Karczewski, Phys. Rev. Lett. **99**, 026403 (2007).
[9] D. Frustaglia, J. König, and A. H. MacDonald, Phys. Rev. B **70**, 045205 (2004).
[10] K. V. Kavokin, Phys. Rev. B **59**, 9822 (1999).
[11] D. Scalbert, F. Teppe, M. Vladimirova, S. Tatarenko, J. Cibert, and M. Nawrocki, Phys. Rev. B **70**, 245304 (2004).
[12] C. Kehl, G. V. Astakhov, K. V. Kavokin, Yu. G. Kusrayev, W. Ossau, G. Karczewski, T. Wojtowicz, and J. Geurts, Phys. Rev. B **80**, 241203 (2009).
[13] F. Teppe, M. Vladimirova, D. Scalbert, T. Wojtowicz, and J. Kossut, Phys. Rev. B **67**, 033304 (2003).
[14] F. J. Teran, M. Potemski, D. K. Maude, D. Plantier, A. K. Hassan, A. Sachrajda, Z. Wilamowski, J. Jaroszynski, T. Wojtowicz, and G. Karczewski, Phys. Rev. Lett. **91**, 077201 (2003).
[15] J. König and A. H. MacDonald, Phys. Rev. Lett. **91**, 077202 (2003).
[16] M. Vladimirova, S. Cronenberger, P. Barate, D. Scalbert, F. J. Teran, and A. P. Dmitriev, Phys. Rev. B **78**, 081305(R) (2008).
[17] C. Attaccalite, S. Moroni, P. Gori-Giorgi, and G. B. Bachelet, Phys. Rev. Lett. **88**, 256601 (2002).
[18] J. A. Gaj, R. Planel, and G. Fishman, Solid State Commun. **29**, 435 (1979).
[19] A. Haury, A. Wasiela, A. Arnoult, J. Cibert, S. Tatarenko, T. Dietl, and Y. Merle d'Aubigné, Phys. Rev. Lett. **79**, 511 (1997).
[20] C. Aku-Leh, F. Perez, B. Jusserand, D. Richards, W. Pacuski, P. Kossacki, M. Menant, and G. Karczewski, Phys. Rev. B **76**, 155416 (2007).
[21] S. A. Crooker, D. D. Awschalom, J. J. Baumberg, F. Flack, and N. Samarth, Phys. Rev. B **56**, 7574 (1997).
[22] C. Camilleri, F. Teppe, D. Scalbert, Y. G. Semenov, M.

Nawrocki, M. Dyakonov, J. Cibert, S. Tatarenko, and T. Wojtowicz, Phys. Rev. B **64**, 085331 (2001).
[23] A. A. Sirenko, T. Ruf, M. Cardona, D. R. Yakovlev, W. Ossau, A. Waag, and G. Landwehr, Phys. Rev. B **56**, 2114 (1997).
[24] D. M. Wang, Y. H. Ren, X. Liu, J. K. Furdyna, M. Grimsditch, and R. Merlin, Phys. Rev. B **75**, 233308 (2007).
[25] M. Scheibner, T. A. Kennedy, L. Worschech, A. Forchel, G. Bacher, T. Slobodskyy, G. Schmidt, and L. W. Molenkamp, Phys. Rev. B **73**, 081308(R) (2006).
[26] Y. G. Semenov, Phys. Rev. B **67**, 115319 (2003).
[27] S. Cronenberger, P. Barate, A. Brunetti, M. Vladimirova, D. Scalbert, F. J. Teran, G. Karzewski, and T. Wojtowicz, Superlattices Microstruct. **43**, 427 (2008).
[28] B. A. Piot, D. K. Maude, M. Henini, Z. R. Wasilewski, K. J. Friedland, R. Hey, K. H. Ploog, A. I. Toropov, R. Airey, and G. Hill, Phys. Rev. B **72**, 245325 (2005).
[29] J. Zhu, H. L. Störmer, L. N. Pfeiffer, K. W. Baldwin, and K. W. West, Phys. Rev. Lett. **90**, 056805 (2003).
[30] B. A. Piot, D. K. Maude, U. Gennser, A. Cavanna, and D. Mailly, Phys. Rev. B **80**, 115337 (2009).
[31] Y. Zhang and S. Das Sarma, Phys. Rev. Lett. **96**, 196602 (2006).
[32] T. Dietl, A. Haury, and Y. Merle d'Aubigné, Phys. Rev. B **55**, R3347 (1997).
[33] S. De Palo, M. Botti, S. Moroni, and Gaetano Senatore, Phys. Rev. Lett. **94**, 226405 (2005).
[34] M. M. Fogler and B. I. Shklovskii, Phys. Rev. B **52**, 17366 (1995).